Nuclear Structure Effects in Muonic Atom Spectroscopy

Chen Ji
Central China Normal University
Institute of Particle Physics

MIP 2026, Huizhou

Atomic precision spectroscopy probes nuclear structure

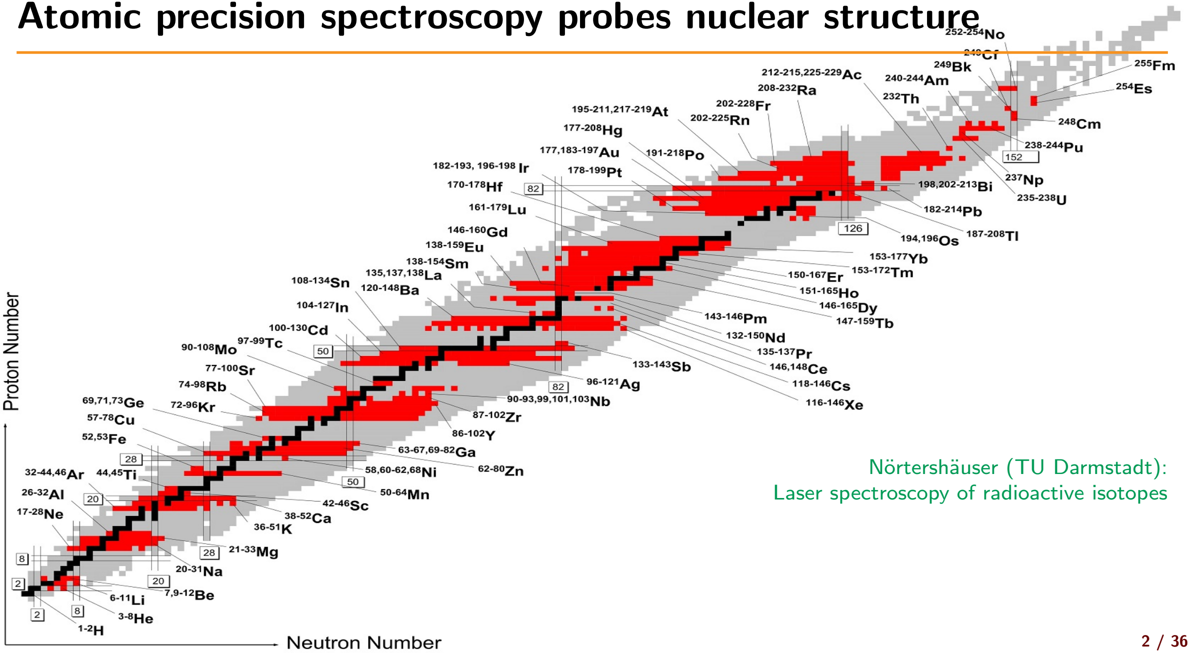

Nörtershäuser (TU Darmstadt):
Laser spectroscopy of radioactive isotopes

Nuclear structure in atomic precision spectroscopy

- Atomic spectroscopy provides rich nuclear structure information
  - Observables: spin, charge radius, magnetic moment, electric quadrupole moment, magnetic radius.
  - Kinematics: shell evolution, β-stability line, drip lines, halo structure, deformation.
- Precision measurements help constrain nuclear force models and many-body theories
  - Determining tensor forces, meson-exchange currents, three-body forces, etc.

Proton radius puzzle

- Electron–proton experiments: $r_p = 0.8770(45)$ fm
  - eH atomic spectroscopy
  - e–p elastic scattering
- Muon–proton experiments: $r_p = 0.8409(4)$ fm
  - μH atom Lamb shift (ΔE_{2S-2P}) [PSI-CREMA]
    Pohl *et al.*, Nature (2010); Antognini *et al.*, Science (2013)

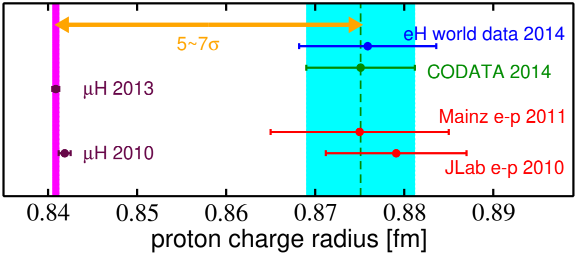

Resolving the proton radius puzzle

- New experiments to measure the proton radius
  - $e-p$ scattering (JLab, Mainz, Tohoku U.)
  - $\mu-p$ scattering (PSI-MUSE)
  - eH spectroscopy (MPQ, LKB, York U.)

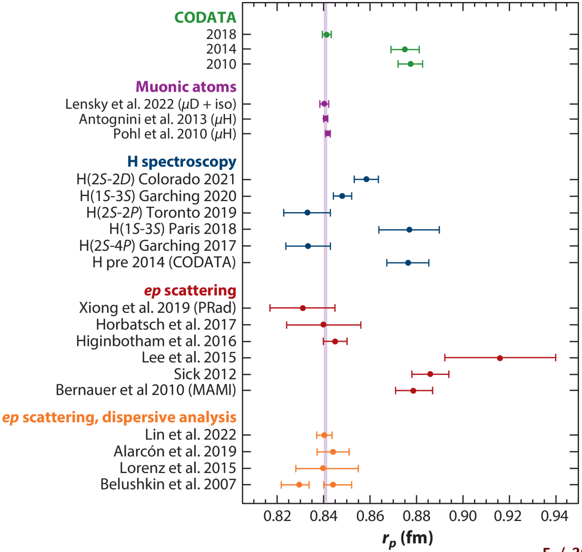

Nuclear charge radii from other atomic precision spectroscopy

- Muonic atoms/ions: Lamb shift spectroscopy (PSI-CREMA)
  - $\mu^2\mathrm{H}$ [Pohl *et al.*, Science 2016]
  - $\mu^4\mathrm{He}^+$ [Krauth *et al.*, Nature 2021]
  - $\mu^3\mathrm{He}^+$ [K. Schuhmann *et al.*, Science 2025]

- Few-electron atomic systems: isotope shift spectroscopy
  - $e^{1-2}\mathrm{H}$ [Parthey *et al.* 2010; Jentschura *et al.* 2011]
  - $e^{3-4}\mathrm{He}$ [Shiner; Cancio Pastor; van Rooij; Zheng; van der Werf]
  - $e^{4-6,8}\mathrm{He}$ [Wang *et al.* 2004; Mueller *et al.* 2007]
  - $e^{7-6,8,9,11}\mathrm{Li}$ [Ewald *et al.* 2004; Sánchez *et al.* 2006]

QUARTET experiment: high-precision X-ray spectroscopy

- Technique: magnetic microcalorimeters to measure X-rays
- Advantages: broad energy bandwidth, high resolution, high detection efficiency
- Goal: improve charge-radius precision for light nuclei from Li to Ne

Isot.	E_{1S-2P} keV	δ_{exp} eV	δ_{NP} eV	fm/keV	δ_r 10^{-3} fm	Gain	Good for
^{11}B	52	$5 \to 0.10$	$0.2 \to 0.05$	-6.7	$21 \to 0.8$	26	Mir., HLI, Chain
^{9}Be	33	$10 \to 0.07$	$0.1 \to 0.03$	−16	$12 \to 1.3$	9	Mir., HLI, Chain
^{7}Li	19	$60 \to 0.05$	$0.03 \to 0.01$	−47	$42 \to 2.4$	17	Mir., Chain

Isot.	E_{1S-2P} keV	δ_{exp} eV	δ_{NP} eV	fm/keV	δ_r 10^{-3} fm	Gain	Good for
^{12}C	75	$0.5 \to 0.15$	$0.3 \to 0.15$	-3.2	$1.9 \to 0.7$	3	χPT, HLI
^{11}B	52	$5 \to 0.10$	$0.2 \to 0.05$	-6.7	$21 \to 0.8$	26	Mir., HLI, Chain
^{9}Be	33	$10 \to 0.07$	$0.1 \to 0.03$	−16	$12 \to 1.3$	9	Mir., HLI, Chain

Pair	ΔE_{2P-1S} eV	δ_{exp} eV	δ_{NP} eV	fm/keV	$\delta_{\Delta r}$ 10^{-3}fm	Gain	Good for
^{20,22}Ne	230	$6 \to 0.5$	$2 \to 0.5$	-0.4	$4.3 \to 0.4$	11	Δg
^{16,18}O	28	$10 \to 0.2$	$0.7 \to 0.3$	-1.0	$9.8 \to 0.3$	33	Δg

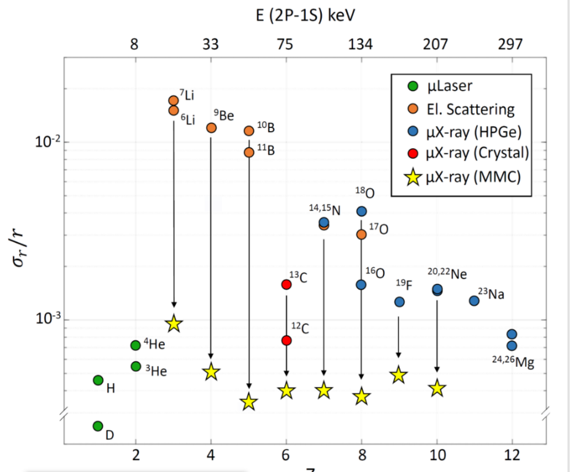

QUARTET Research Proposal

Nuclear structure in atomic Lamb shift spectroscopy

- Extracting nuclear charge radii from muonic atom Lamb shift

$$\delta E_{\rm LS} = \delta_{\rm QED} + \mathcal{A}_{\rm OPE}\, R_E^2 + \delta_{\rm TPE}$$

- **QED corrections:**
  - Vacuum polarization
  - Lepton self-energy corrections
  - Relativistic recoil corrections

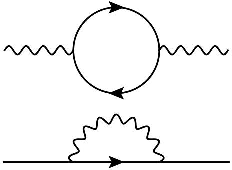

Nuclear structure in atomic Lamb shift spectroscopy

- Extracting nuclear charge radii from muonic atom Lamb shift

$$\delta E_{\rm LS} = \delta_{\rm QED} + \boxed{\mathcal{A}_{\rm OPE}\, R_E^2} + \delta_{\rm TPE}$$

- **Nuclear structure corrections:**
  - $\propto R_E^2 \Longrightarrow$ **nuclear structure in one-photon exchange**
    $\mathcal{A}_{\rm OPE} \approx m_\mu^3 (Z\alpha)^4/12$

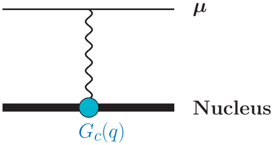

Nuclear structure in atomic Lamb shift spectroscopy

- Extracting nuclear charge radii from muonic atom Lamb shift

$$\delta E_{\rm LS} = \delta_{\rm QED} + \mathcal{A}_{\rm OPE}\, R_E^2 + \boxed{\delta_{\rm TPE}}$$

- **Nuclear structure corrections:**
  - $\boldsymbol{\delta_{\rm TPE}} \Longrightarrow$ **nuclear structure in two-photon exchange**
    - Elastic contribution: Zemach moment $\delta_{\rm Zem}$
    - Inelastic contribution: nuclear polarizability $\delta_{\rm pol}$

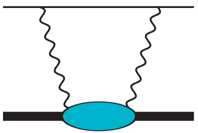

- **Accuracy of extracted nuclear radius R_E depends on theoretical input of $\delta_{\rm TPE}$**

  μ^2H experiment: $\delta_{\rm pol}$ requires 1% theoretical precision

  $\mu^{3,4}$He$^+$ experiments: $\delta_{\rm pol}$ requires 5% theoretical precision

Nuclear polarizability from photonuclear sum rules

$$\delta_{\rm pol} = \sum_{g,\, S_{\hat{O}}} \int_{\omega_{th}}^{\infty} d\omega \underbrace{g(\omega)}_{\text{weight}} \underbrace{S_{\hat{O}}(\omega)}_{\text{nuclear response function}}$$

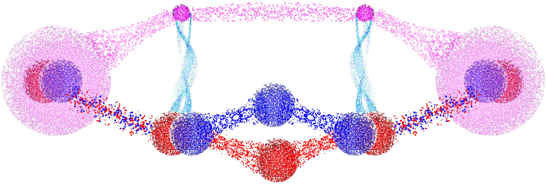

- Energy sum-rule weight $g(\omega)$
- Nuclear response function $S_{\hat{O}}(\omega)$

$$S_O(\omega) = \sum\!\!\!\!\!\!\!\int_f |\langle\psi_f|\hat{O}|\psi_0\rangle|^2 \delta(E_f - E_0 - \omega)$$

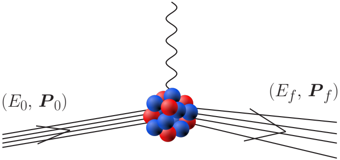

Nuclear polarizability from photonuclear sum rules

$$\delta_{\rm pol} = \sum_{g,\, S_{\hat{O}}} \int_{\omega_{th}}^{\infty} d\omega\, \underbrace{g(\omega)}_{\text{weight}}\, \underbrace{S_{\hat{O}}(\omega)}_{\text{nuclear response function}}$$

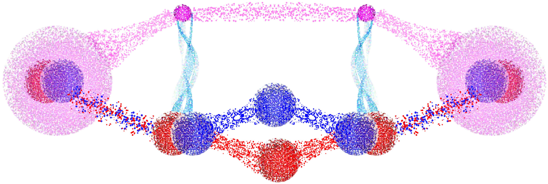

Contributions to nuclear polarizability $\delta_{\rm pol}$ in muonic atoms:

- Electromagnetic multipole expansion
  - E0, E1, E2 response sum rules
- Relativistic and Coulomb distortion corrections
- Intrinsic nucleon structure corrections

CJ, Bacca, Barnea, Hernandez, Nevo-Dinur, JPG 45, 093002 (2018)

Nuclear response function: continuum spectrum

- The nucleus is virtually excited in two-photon exchange

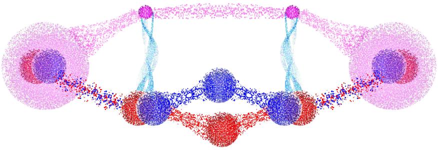

$$S_O(\omega) = \sum\!\!\!\!\!\!\!\int_f |\langle \psi_f | \hat{O} | \psi_0 \rangle|^2 \delta(E_f - E_0 - \omega)$$

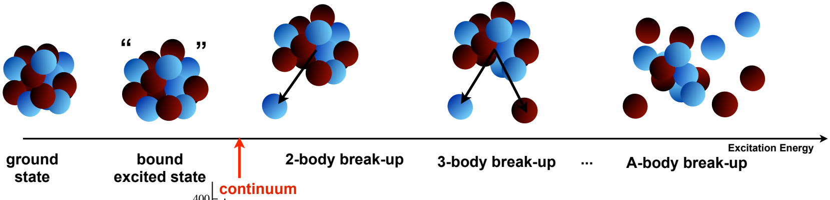

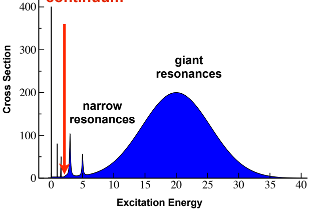

$$\sigma \propto \left| \langle \Psi_f | J^\mu | \Psi_0 \rangle \right|^2$$

Exact knowledge limited in energy and mass number

Ab initio calculations of nuclear polarizability $\delta_{\rm pol}$

- $\mu^{2,3}$H, $\mu^{3,4}$He$^+$:
  - Ab initio numerical methods
    Effective Interaction Hyperspherical Harmonics (EIHH)
    Lorentz Integral Transform (nuclear response functions)
    Lanczos Algorithm (sum rules)
    bound states $\rightarrow$ resonance/scattering states
  - Nucleon–nucleon interactions
    AV18+UIX
    χEFT NN(N^{3}LO)+NNN(N^{2}LO)
    $\not\pi$EFT (N^{2}LO)
    Compare $\delta_{\rm pol}$ from different nuclear force models to estimate nuclear theory uncertainties

CJ, Nevo-Dinur, Bacca, Barnea, PRL 111, 143402 (2013)
Hernandez, CJ, Bacca, Nevo-Dinur, Barnea, PLB 736, 344 (2014)
Nevo Dinur, CJ, Bacca, Barnea, PLB 755, 380 (2016)
Hernandez, Ekström, Nevo Dinur, CJ, Bacca, Barnea, PLB 788, 377 (2018)
CJ, Bacca, Barnea, Hernandez, Nevo-Dinur, JPG 45, 093002 (2018)
Hernandez, Ekström, Nevo, CJ, Bacca, Barnea, PLB 788, 377 (2018)
Nevo, Hernandez, Bacca, Barnea, CJ, Pastore, Piarulli, Wiringa, PRC 99, 034004 (2019)
Emmons, CJ, Platter, JPG 48, 035101 (2021)
CJ, Zhang, Platter, PRL 133, 042502 (2024)
Bonilla, Richardson, Bacca, CJ, Platter, PLB 874, 140257 (2026)

Nuclear theory uncertainties in two-photon exchange

$\delta_{\rm TPE}$ in $\mu\,^3$He$^+$

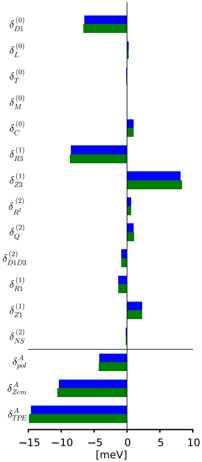

	AV18/UIX	χEFT
$\delta^{(0)}_{D1}$	-6.479	-6.633
$\delta^{(0)}_{L}$	0.232	0.240
$\delta^{(0)}_{T}$	-0.103	-0.107
$\delta^{(0)}_{M}$	0.006	0.006
$\delta^{(0)}_{C}$	1.000	1.020
$\delta^{(1)}_{R3}$	-8.539	-8.711
$\delta^{(1)}_{Z3}$	8.100	8.327
$\delta^{(2)}_{R^2}$	0.632	0.654
$\delta^{(2)}_{Q}$	1.015	1.038
$\delta^{(2)}_{D1D3}$	-0.841	-0.862
$\delta^{(1)}_{R1}$	-1.294	-1.314
$\delta^{(1)}_{Z1}$	2.256	2.291
$\delta^{(2)}_{NS}$	-0.193	-0.199
δ^{A}_{pol}	-4.208	-4.250
δ^{A}_{Zem}	-10.356	-10.618
δ^{A}_{TPE}	-14.564	-14.868

$\delta_{\rm TPE} = -14.72$ meV $\pm 1.5\% (1\sigma)$

$\delta_{\rm TPE}$ in $\mu\,^4$He$^+$

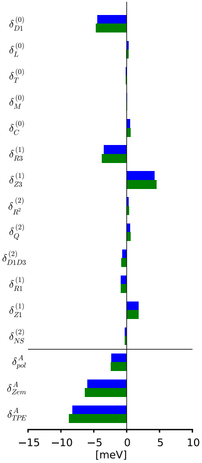

	AV18/UIX	χEFT
$\delta^{(0)}_{D1}$	-4.418	-4.701
$\delta^{(0)}_{L}$	0.289	0.308
$\delta^{(0)}_{T}$	-0.126	-0.134
$\delta^{(0)}_{M}$	0.008	0.006
$\delta^{(0)}_{C}$	0.519	0.553
$\delta^{(1)}_{R3}$	-3.442	-3.717
$\delta^{(1)}_{Z3}$	4.183	4.526
$\delta^{(2)}_{R^2}$	0.259	0.324
$\delta^{(2)}_{Q}$	0.484	0.561
$\delta^{(2)}_{D1D3}$	-0.666	-0.784
$\delta^{(1)}_{R1}$	-0.848	-0.874
$\delta^{(1)}_{Z1}$	1.753	1.811
$\delta^{(2)}_{NS}$	-0.279	-0.293
δ^{A}_{pol}	-2.284	-2.414
δ^{A}_{Zem}	-5.936	-6.337
δ^{A}_{TPE}	-8.220	-8.751

$\delta^{A}_{\rm TPE} = -8.49$ meV $\pm 4.4\% (1\sigma)$

Charge radii from μ^2H and μ^4He$^+$ Lamb shift

- Nuclear polarizability predictions used by PSI experiments to extract nuclear radii
- Uncertainty of extracted charge radii is dominated by nuclear polarizability theory uncertainty

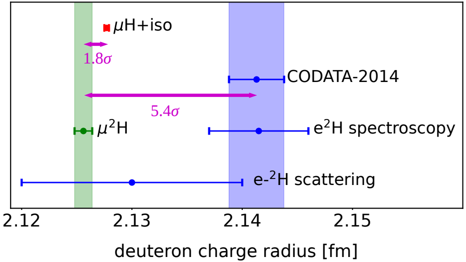

$$r_d = 2.12562(13)_{\rm exp}(77)_{\rm theo}\ \text{fm}$$

Pohl, *et al.*, Science (2016)

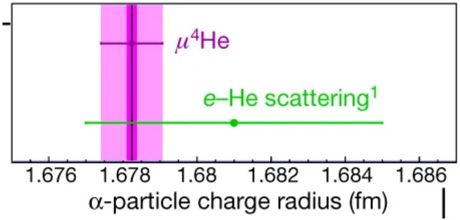

$$r_\alpha = 1.67824(13)_{\rm exp}(82)_{\rm theo}\ \text{fm}$$

Krauth et al., Nature (2021)

Nuclear polarizability theory:

Hernandez, CJ, Bacca, Nevo-Dinur, Barnea, PLB 736, 344 (2014); PRC 100, 064315 (2019) (μ^2H)

Hernandez, Ekström, Nevo Dinur, CJ, Bacca, Barnea, PLB 788, 377 (2018) (μ^2H)

CJ, Nevo-Dinur, Bacca, Barnea, PRL 111, 143402 (2013) (μ^4He$^+$)

CJ, Bacca, Barnea, Hernandez, Nevo-Dinur, JPG 45, 093002 (2018) ($\mu^{2,3}$H, $\mu^{3,4}$He$^+$)

Charge radius from μ^3He$^+$ Lamb shift

- Nuclear polarizability predictions used by PSI experiments to extract nuclear radii
- Uncertainty of extracted charge radii is dominated by nuclear polarizability theory uncertainty

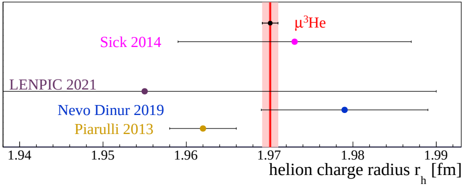

$r_h = 1.97007(12)_{\rm exp}(93)_{\rm theo}$ fm

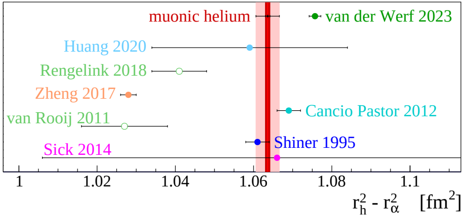

$r_h^2 - r_\alpha^2 = 1.0636(6)_{\rm exp}(30)_{\rm theo}$ fm^2

Schuhmann et al. (CREMA) Science (2025)

Nuclear polarizability theory:
Nevo Dinur, CJ, Bacca, Barnea, PLB 755, 380 (2016) (μ^3H, μ^3He$^+$)
CJ, Bacca, Barnea, Hernandez, Nevo-Dinur, JPG 45, 093002 (2018) ($\mu^{2,3}$H, $\mu^{3,4}$He$^+$)

Effective Zemach radius from atomic HFS

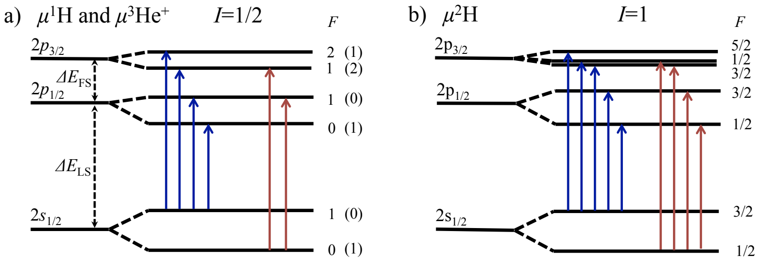

- Zemach radius R_Z is determined by both nuclear charge and magnetization distributions

$$
\begin{aligned}
R_Z &= \iint d\boldsymbol{r} d\boldsymbol{r}' \rho_E(\boldsymbol{r})\, \rho_M(\boldsymbol{r}')\, |\boldsymbol{r}-\boldsymbol{r}'| \\
&= -\frac{4}{\pi}\int_0^\infty \frac{dq}{q^2}\left[G_E(q)G_M(q)-1\right]
\end{aligned}
$$

$\neq$ effective Zemach radius from HFS

Discrepancy in studies of nuclear magnetization form factor

- ^{3}**He** charge form factor F_C: experiment agrees with theory
- ^{3}**He** magnetic form factor F_M: discrepancy between experiment and theory at high momentum
- Muonic atom spectroscopy provides more precise measurements of nuclear magnetization distribution

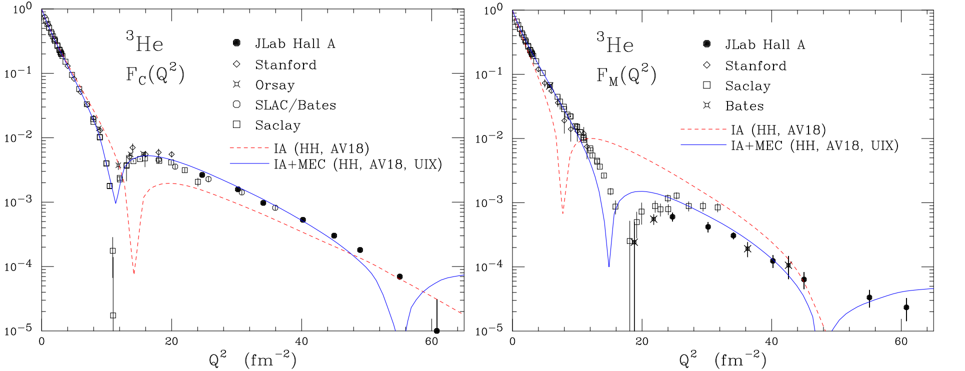

Nuclear effects in atomic HFS: challenges

- Lack of systematic studies of nuclear effects in hyperfine spectra
  - How does nuclear polarizability scale with Z and A?

- In the absence of direct calculations, extract nuclear polarizability via:
  - HFS spectroscopy $-$ QED theory $\rightarrow$ nuclear effects (effective Zemach radius $\tilde{R}_Z$)
  - Form factors from electron–nucleus scattering: compute Zemach radius R_Z
  - $\tilde{R}_Z - R_Z$: nuclear polarizability

Effective Zemach radius: p and d

- HFS spectroscopy → effective Zemach radius $\tilde{R}_Z$:

$$\nu_{\rm TPE} = \nu_{\rm exp} - \nu_{\rm QED} = -2Z\alpha m_R E_F \tilde{R}_Z; \qquad m_R = \frac{m_l m_{nucl}}{m_l + m_{nucl}}$$

	$\nu_{\rm TPE} = \nu_{\rm exp} - \nu_{\rm QED}$	$\tilde{R}_Z$ [fm]	R_Z [fm]	$\Delta\%$
$e\mathrm{H}_{1S}$	-47.4(1) kHz	0.883(2)	1.054(3)	-16%
$\mu\mathrm{H}_{1S}$	-1.161(2) meV	0.906(2)		-14%
$e^2\mathrm{H}_{1S}$	45.2 kHz	-3.66	2.593(16)	-240%
$\mu^2\mathrm{H}_{2S}$	0.0966(73) meV	-2.13(16)		-180%

- $e^2\mathrm{H}_{1S}$: Wineland, Ramsey, PRA (1972)
- $\mu^2\mathrm{H}_{2S}$: Krauth *et al.*, Ann. Phys. 366, 168 (2016); Pohl *et al.*, Science 353, 669 (2016)

Effective Zemach radius: ^{3}He and ^{9}Be

- HFS spectroscopy → effective Zemach radius $\tilde{R}_Z$

	$\nu_{\rm TPE} = \nu_{\rm exp} - \nu_{\rm QED}$	$\tilde{R}_Z$ [fm]	R_Z [fm]	Δ%
$e^3\mathrm{He}^+_{1S}$	1701.0(5.5) kHz	2.600(8)	2.528(16)	3%
$\mu^3\mathrm{He}^+_{2S}$	6.25(10) meV	2.42(39)		-4%
$e^9\mathrm{Be}^+_{1S}$		4.03(5)	3.38(6)	19%
$e^9\mathrm{Be}^{3+}_{1S}$		4.048(2)		20%

- $e^3\mathrm{He}^+_{1S}$: Schneider *et al.*, Nature 606, 878 (2022); Patkóš, Yerokhin, Pachucki, PRA 107, 052802 (2023)
- $\mu^3\mathrm{He}^+_{2S}$: Schuhmann *et al.*, Science 388, 854 (2025); Franke *et al.*, EPJD 71, 341 (2017)
- $e^9\mathrm{Be}^+_{1S}$ & $e^9\mathrm{Be}^{3+}_{1S}$: Puchalski, Pachucki, PRA 89, 032510 (2014); Dickopf *et al.*, Nature 632, 757 (2024)

Effective Zemach radius: ^{6}Li and ^{7}Li

- ^{7}Li: $\tilde{R}_Z$ from HFS agrees with R_Z from nuclear models
- ^{6}Li: large discrepancy between $\tilde{R}_Z$ and R_Z
- Nuclear polarizability: $\delta_{pol}(^7\text{Li}) \ll \delta_{pol}(^6\text{Li})$?

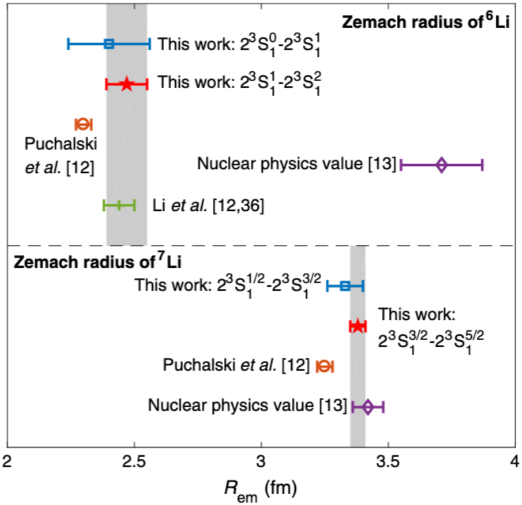

Puchalski, Pachucki, PRL 111, 243001 (2013)
Qi et al., PRL 125, 183002 (2020)
Li et al., PRL 124, 063002 (2020)
Guan et al., PRA 102, 030801(R) (2020)
Sun et al., PRL 131, 103002 (2023)
Nuclear model: Yerokhin PRA 78, 012513 (2008)

Nuclear structure effects in hyperfine splitting spectra

- Extracting Zemach radius from e/μ atom HFS

$$E_{\mathrm{HFS}}(nS) = E_F(1 + \delta_{\mathrm{QED}} + \delta_{\mathrm{TPE}})$$

- Fermi contact term
  - Nuclear–lepton spin coupling

$$E_F = \frac{2\pi\alpha g_m}{3m_\ell m_N}\phi_n^2(0)\langle\vec{\sigma}^{(\ell)}\cdot\vec{I}\rangle$$

- QED corrections
  - Vacuum polarization
  - Lepton self-energy
  - Relativistic recoil
- Two-photon exchange (nuclear structure effects)
  - Nuclear polarizability
  - Elastic contribution (Zemach radius)

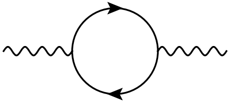

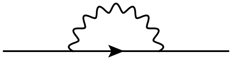

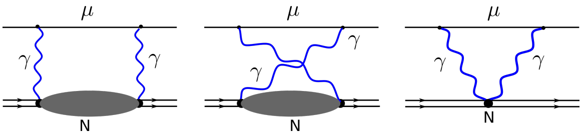

Two-photon corrections in ^{2}H and μ^2H hyperfine spectra

- Two-photon exchange corrections

$$E_{\text{TPE}} = E_{\text{el}} + E_{\text{pol}} + E_{\text{1N}}$$

- Elastic part: $F_c(q)$, $F_m(q)$, $F_Q(q)$: $\sim r_Z$
- Inelastic vector polarizability
- E_{1N}: single-nucleon TPE (nucleon structure)

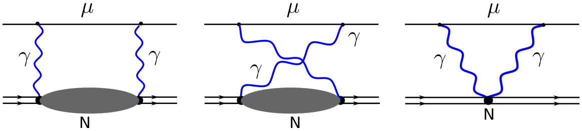

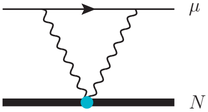

$$\delta_{\text{pol}}^{(0,1)} \propto \int d\omega \int dq h^{(0,1)}(\omega, q) S^{(0,1)}(\omega, q)$$

Charge–magnetization current coupling:

$$S^{(0)}(\omega, q) = -\frac{1}{q^2} \text{Im} \sum\!\!\!\!\!\!\!\int_{N \neq N_0} \int \frac{d\hat{q}}{4\pi} \langle N_0 II | \left[\vec{q} \times \vec{J}_m^\dagger(\vec{q}) \right]_3 | N \rangle \langle N | \rho(\vec{q}) | N_0 II \rangle \, \delta\left(\omega - \frac{q^2}{2m_A} - \omega_N \right)$$

Convection–magnetization current coupling:

$$S^{(1)}(\omega, q) = -\text{Im} \sum\!\!\!\!\!\!\!\int_{N \neq N_0} \int \frac{d\hat{q}}{4\pi} \epsilon^{3jk} \langle N_0 II | \vec{J}_{m,j}^\dagger(\vec{q}) | N \rangle \langle N | \vec{J}_{c,k}(\vec{q}) | N_0 II \rangle \, \delta\left(\omega - \frac{q^2}{2m_A} - \omega_N \right)$$

Polarizability response functions for HFS TPE

- $S^{(0)}(\omega, q)$: charge-density to magnetization-current transition (LO)
- $S^{(1)}(\omega, q)$: convection-current to magnetization-current transition (NLO)
- $S^{(0)}_{\mathrm{sd}}(\omega, q)$: SD-coupling correction (NNLO)
- Nuclear response functions converge order by order

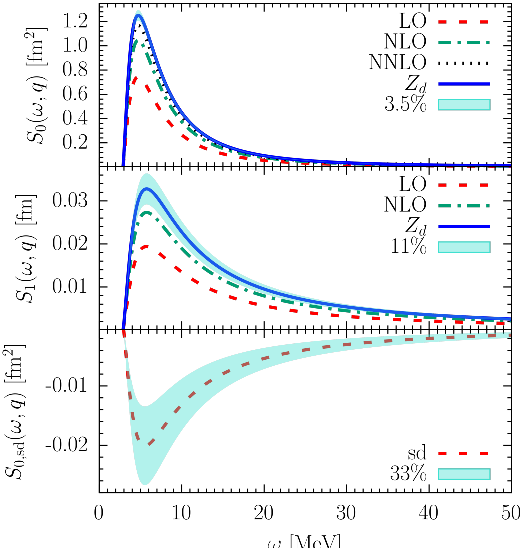

CJ*, Zhang, Platter, PRL 133, 042502 (2024)

^{2}H and μ^2H HFS two-photon corrections (pionless EFT)

	^{2}H (1S)	μ^2H (1S)	μ^2H (2S)
$E_{1\mathrm{p}}$ (Antognini 2022)	$-35.54(8)$	$-1.018(2)$	$-0.1272(2)$
$E_{1\mathrm{n}}$ (Tomalak 2019)	$9.6(1.0)$	$0.08(3)$	$0.010(4)$
E_{el}	$-42.1(2.1)$	$-0.984(46)$	$-0.123(6)$
E_{pol}	$109.8(4.5)$	$2.86(12)$	$0.358(14)$
E_{TPE}	kHz	meV	meV
This work	$41.7(4.4)$	$0.94(11)$	$0.117(13)$
Khriplovich, Milstein 2004	43		
Friar, Payne 2005 $_{\mathrm{mod}}$	64.5		
Kalinowski, Pachucki 2018		$0.304(68)$	$0.0383(86)$
$\nu_{\mathrm{exp}} - \nu_{\mathrm{qed}}$	45.2		$0.0966(73)$

- Calculations explain the experiment–QED discrepancy within $0.8 - 1.3\sigma$
- Theoretical uncertainty of single-nucleon corrections may be underestimated (ChPT and dispersion-relation calculations differ by a factor of 10)

CJ*, Zhang, Platter, PRL 133, 042502 (2024)

Nuclear response functions from χEFT (convergence analysis)

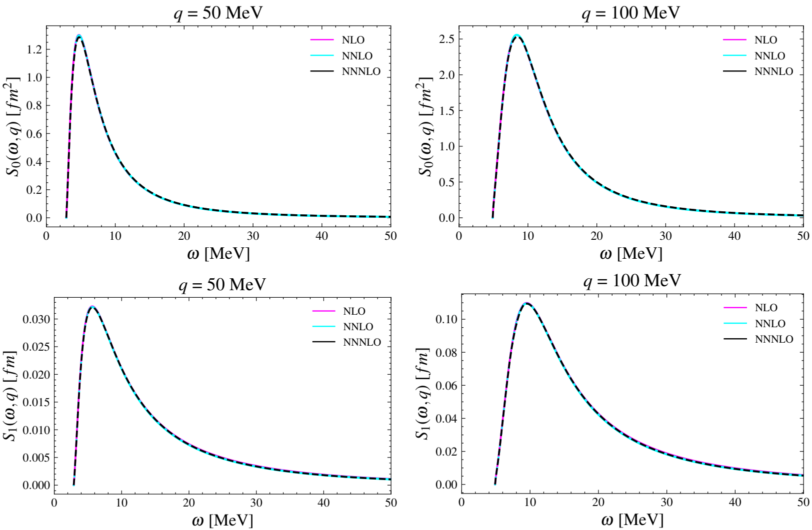

Bonilla, Richardson, Bacca, CJ, Platter, arXiv:2508.18776

Nuclear response functions from χEFT (partial-wave analysis)

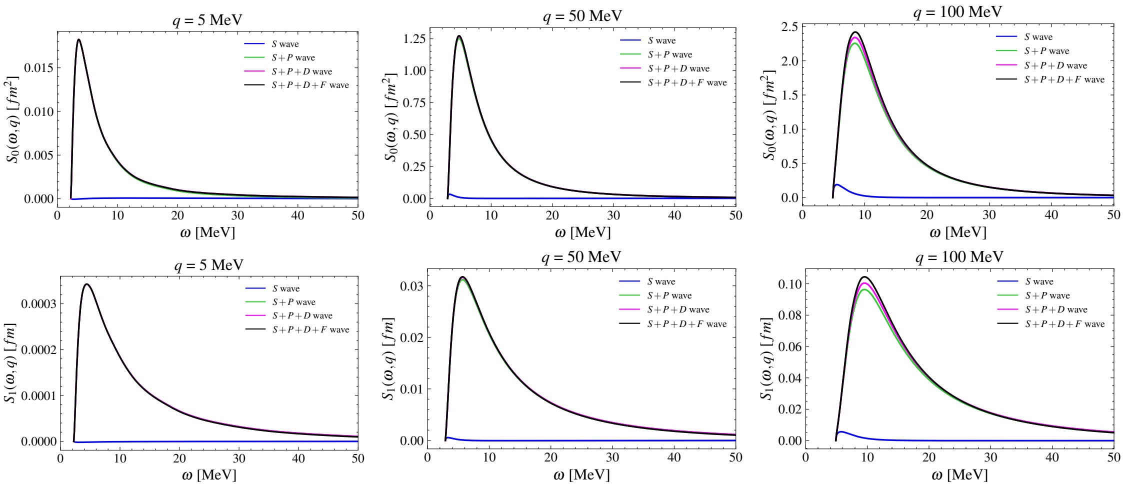

Bonilla, Richardson, Bacca, CJ, Platter, PLB 874, 140257 (2026)

^{2}H, μ^2H HFS polarizability: χEFT vs $\not\pi$EFT

	e^2H (1S) [kHz]	μ^2H (1S) [meV]	μ^2H (2S) [meV]
$\nu_{\rm EXP} - \nu_{\rm QED}$	45	-	0.0966(73)
$\Delta_{2\gamma}$ ($\not\pi$EFT)	41.7(2.6)	0.940(73)	0.118(9)
$\Delta_{2\gamma}$ (χEFT)	44.5(1.1)	0.995(57)	0.124(7)
Khriplovich 2004	43		
Friar 2005	64.5		
Kalinowski, Pachucki 2018		0.304(68)	0.0383(86)

- χEFT prediction of TPE effects agrees with $\not\pi$EFT prediction
- Uncertainty mainly from higher-order χEFT terms and 3γ-exchange contributions

Bonilla, Richardson, Bacca, CJ, Platter, PLB 874, 140257 (2026)

Nuclear effects in other atomic hyperfine spectra

- Exact approach: Lanczos sum rules
  - Nuclear effects in HFS: EM operators and excitation modes more complex than Lamb shift
  - Excited-state calculations converge slowly with large numerical cost

- Approximate approach: closure approximation
  - Zero-excitation-energy approximation $\omega \to 0$ (Low term)

  - Finite-excitation-energy closure:
    - Set $\omega = \bar{\omega}$ as a finite but fixed parameter
    - Apply closure $\sum |N\rangle\langle N| = 1 - |0\rangle\langle 0|$ at fixed $\bar{\omega}$
    - Reduce nuclear polarizability to ground-state observables

Yang, Epelbaum, CJ, Zhao, arXiv:2509.01303

Neural-network variational Monte Carlo

- Use neural networks to optimize parameters of quantum many-body wave functions
- Train the network variationally to minimize the ground-state binding energy
- Use the high-precision ground-state wave function to compute TPE observables

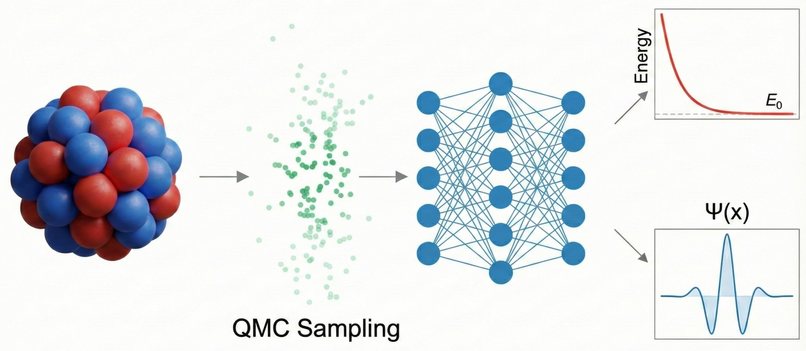

Yang, Epelbaum, CJ, Zhao, arXiv:2509.01303

Effective Zemach radius via closure approximation

- Elastic R_Z: Monte Carlo results agree with experimental extraction from form factors
- Effective Zemach radius ($\tilde{R}_Z$): weak dependence on closure energy (stable for ω: 10–30 MeV)
- Tune $\bar{\omega}$ to best-fit $\tilde{R}_Z$

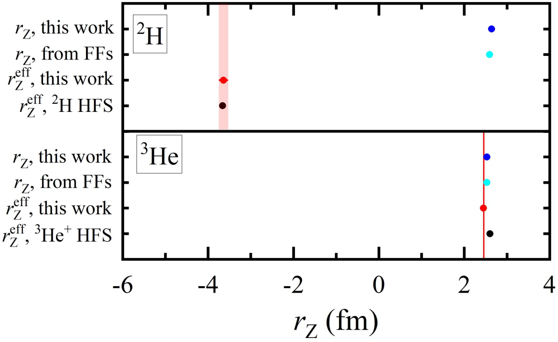

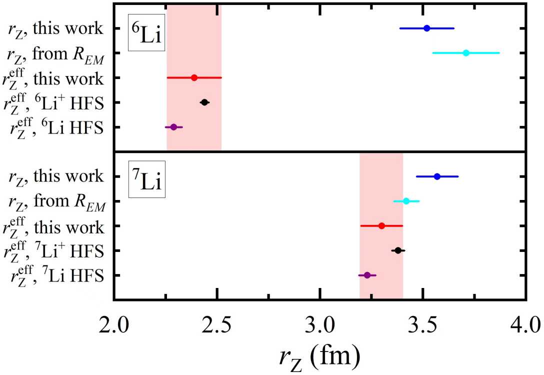

Yang, Epelbaum, CJ, Zhao, arXiv:2509.01303

HFS in muonic helium atom (μe^4He)

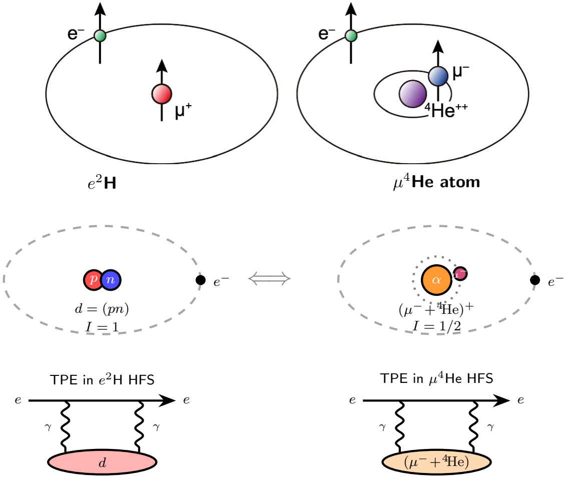

- μe^4He atom: 3-body system ($\mu^- + e^- + {}^4$He)
- Pseudonucleus $[\mu^- + {}^4\text{He}]^+$: tightly bound
  - $|E_\mu| \sim 11$ keV; $a_\mu \approx 132$ fm
  - $I = 1/2$, $g_\mu \approx 2.002$
- Outer e: binding ~ 13.6 eV; scale separation ~ 800
- TPE probes the pseudonucleus structure $\Rightarrow$ analog of e^2H HFS

TPE formalism for μ^4He atom HFS

- Same decomposition as e^2H / μ^2H HFS:

$$E_{\rm TPE} = E_{\rm el} + E_{\rm pol}$$

- Polarizability split into charge–magnetic (0) and magnetic–magnetic (1):

$$\delta_{\rm pol}^{(0,1)} \propto \int d\omega \int dq\; h^{(0,1)}(\omega, q)\, S^{(0,1)}(\omega, q)$$

- Response function for pseudonucleus : intermediate excitation of $\mu^- + {}^4$He

CJ, *et al.*, in preparation

Experimental status of μ^4He atom HFS

- Ground-state HFS frequency $\Delta\nu\,(\mu^4\text{He}) \approx 4465$ MHz

Experiment	$\Delta\nu$ [MHz]	Precision	Reference
SIN (1980, weak field)	$4464.95(6)$	13 ppm	Orth *et al.*, PRL 45, 1483 (1980)
LAMPF (1982, high field)	$4465.004(29)$	6.5 ppm	Gardner *et al.*, PRL 48, 1168 (1982)
J-PARC MuSEUM (2023)	$4464.980(20)$	4.5 ppm	Strasser *et al.*, PRL 131, 253003 (2023)

- J-PARC MuSEUM program:
  - H-line upgrade (1 MW beam, $\sim 10^7\ \mu^-/\text{s}$) $\rightarrow$ target < 100 ppb on $\Delta\nu$
  - Spin-exchange optical pumping (Rb/K SEOP) to re-polarize μHe atoms $\rightarrow$ reach $\mathcal{O}(10)$ ppb
  - Extension to μ^3He atom and $2s$ HFS
- Physics reach: muon magnetic moment μ_{μ^-} and mass m_{μ^-} at sub-ppm, CPT test
- Theory precision on TPE $\Rightarrow$ improve systematic for extracting μ_{μ^-}

Summary

- Proton radius puzzle and atomic precision spectroscopy
  - Challenges to lepton universality and higher-order QED theory
  - Nuclear polarizability connects photonuclear reactions with atomic spectra
  - Probe precision physics with low-energy nuclear structure theory
- Ab initio calculations of nuclear effects in atomic spectra
  - Two-photon exchange correction to muonic-atom Lamb shift
  - Two-photon exchange correction to e^2H, μ^2H, and $e\mu^4$He hyperfine splittings
  - Theoretical input at percent-level precision is more accurate than nuclear polarizability extracted from photonuclear data

CiADS: opportunities for muonic-atom precision spectroscopy

- CiADS (Huizhou) offers new opportunities for muonic-atom precision spectroscopy
  - High-intensity muon source enabling high-precision muonic-atom spectroscopy
  - Study nuclear charge and magnetization distributions
  - Study nuclear polarizability, compare with Compton scattering, test chiral perturbation theory
  - Muonic-atom HFS spectroscopy (μe^4He, μe^3He, ...): complement to J-PARC MuSEUM; bound muon g-factor and mass, CPT test
  - Test bound-state QED
  - Search for symmetry violations

Collaborators

Ab initio muonic-atom Lamb shift

O.J. Hernandez
S. Bacca *(Mainz)*
N. Nevo-Dinur
N. Barnea *(Hebrew U.)*
A. Ekström *(Chalmers)*

Two-nucleon currents

S. Pastore, M. Piarulli *(Wash. U.)*
R.B. Wiringa *(Argonne)*

Pionless EFT

S.B. Emmons *(Carson-Newman)*
L. Platter *(U. Tennessee)*
H. Zhang (CCNU)

χEFT response functions

S. Bacca, J. Richardson *(Mainz)*
A. Bonilla, L. Platter *(U. Tennessee)*

Neural-network VMC

E. Epelbaum *(Bochum)*
H. Yang, P. Zhao *(Peking U)*

Thank you for your attention!